Electronic Supplementary Material (ESI) for Journal of Materials Chemistry

Supporting Information

Self-assembled multilayer of alkyl graphene oxide for highly selective detection of copper(II) based on anodic stripping voltammetry

Wen Zhang,[†ab] Juan Wei,[†a] Houjuan Zhu,[ab] Kui Zhang,[a] Fang Ma,[ab] Qingsong Mei,[a] Zhongping Zhang[ab] and Suhua Wang[*ab]

[a] Institute of Intelligent Machines, Chinese Academy of Sciences, Hefei, Anhui, 230031, China.
[b] Department of Chemistry, University of Science & Technology of China, Hefei, Anhui, 230026, China.
E-mail: shwang@iim.ac.cn

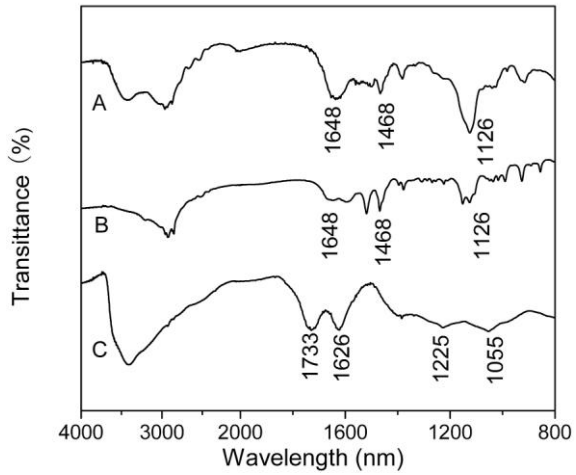

Fig. S1 FT-IR spectra of (A) GO-C3Me, (B) GO-C7Me and (C) GO, showing the amide formation of alkylamine functionalized GO.

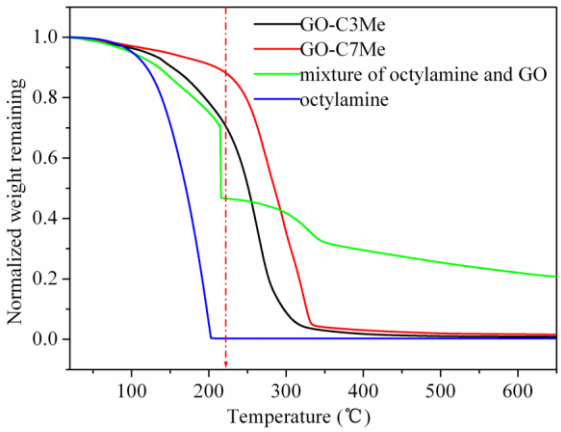

Fig. S2 TGA profiles of pure octylamine, simple mixture of octylamine and GO, GO-C7Me, and GO-C3Me sample. There is only one weight-loss process for both GO-C7Me and GO-C3Me samples, indicating the covalent attachment of alkylamine to GO. There are two weight-loss steps in the simple mixture of octylamine and GO, which can be attributed to the thermal decomposition of octylamine and GO respectively.

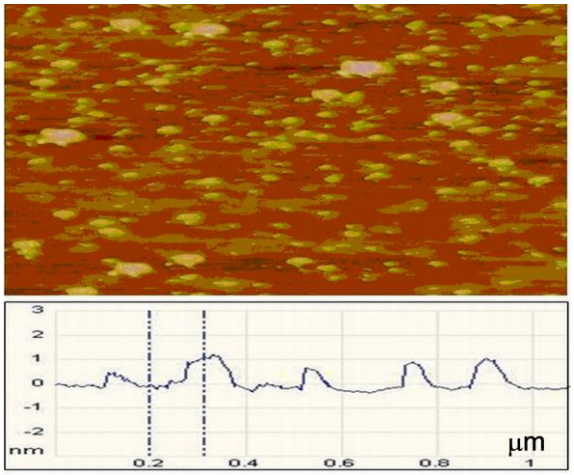

Fig. S3 AFM image and cross-section analysis of single GO-C7Me nanosheets on mica substrate. The thickness of a single GO nanosheet is estimated to be about 1 nm. The unit of the horizontal ordinate is micrometer (μm).

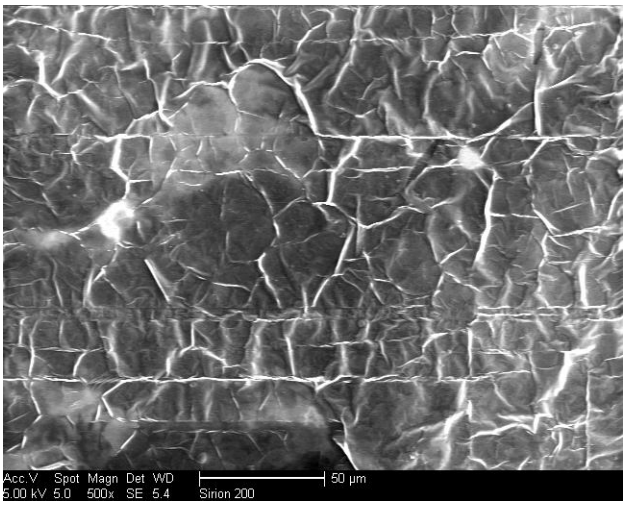

Fig. S4 SEM image of GO-C7Me self-assembled multilayer on amorphous Si substrate.

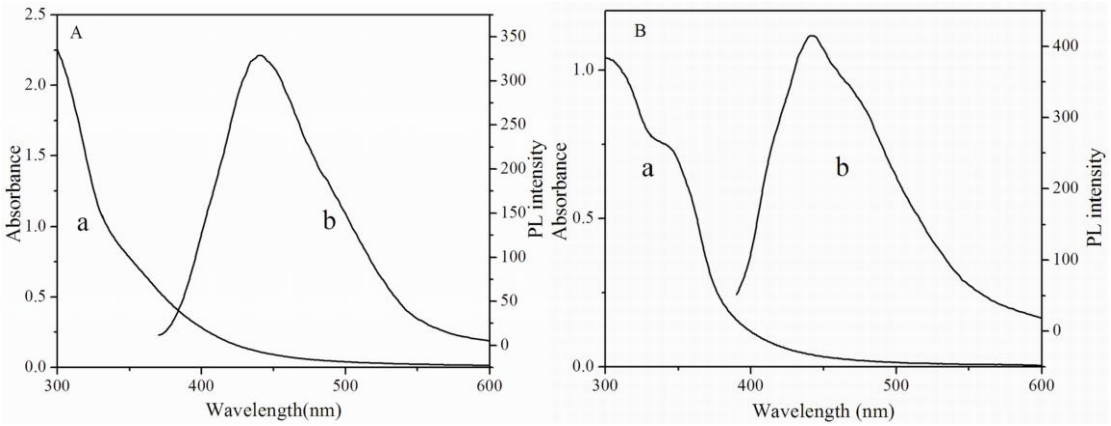

Fig. S5 (A) UV-vis absorption of GO-C3Me in water (3 mg/mL) (a), the fluorescence spectrum of GO-C3Me in water (75 μg/mL) (b); (B) UV-vis absorption of GO-C7Me in ethanol (5 mg/mL) (a), the fluorescence spectrum of GO-C7Me in ethanol (200 μg/mL) (b).

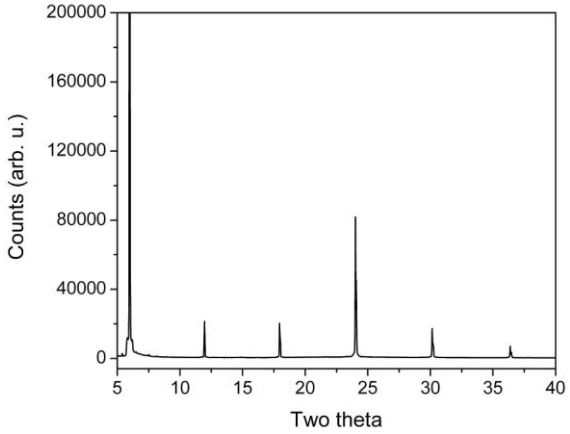

Fig. S6 X-ray diffraction patterns of GO-C3Me on Si substrate**.**

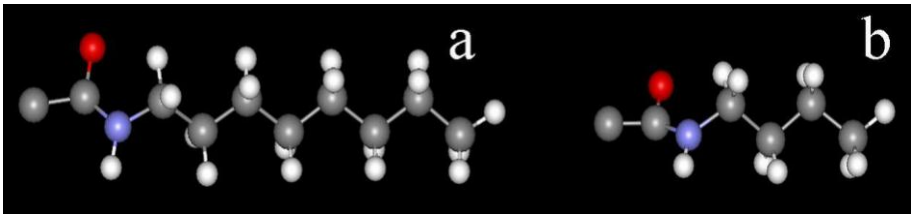

Fig. S7 Simulated length of the molecule chain used in the chemical reaction (a) octylamine, and (b) n-butylamine. Calculation results are summaried in Table S1.

Table S1. Comparison between the interlayer spacing obtained from XRD measurement and computer simulation

	GO-C3Me (nm)	GO-C7Me (nm)
molecular chain length (d_s)	0.857	1.381
$2d_s$	1.714	2.762
interlayer spacing from XRD	1.472	2.255

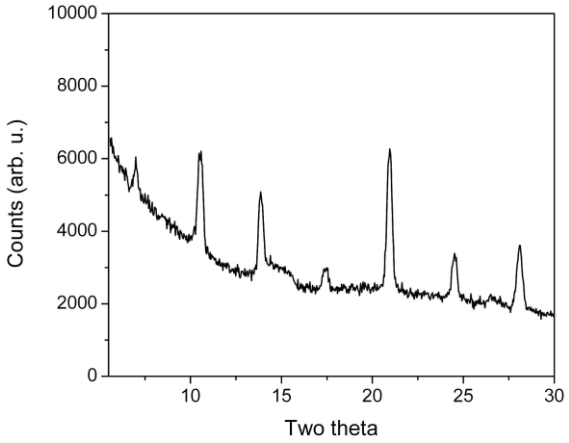

Fig. S8 X-ray diffraction patterns of GO-C7Me self-assembled on Au electrode substrate, showing the same regular ordered structures as on amorphous Si substrate.

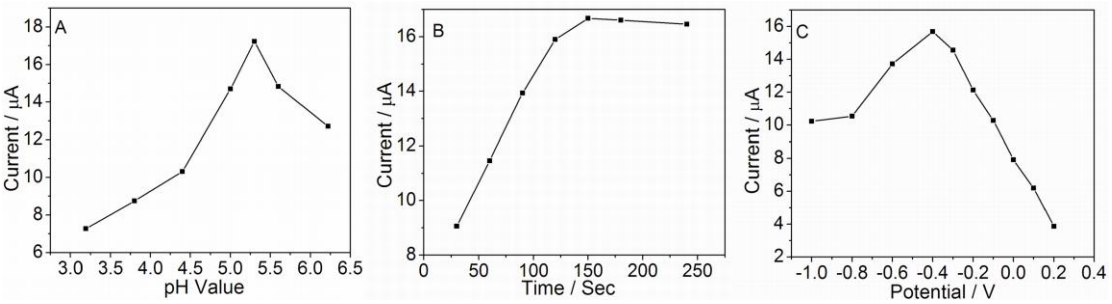

Fig. S9 Effect of different parameters on the peak current of SWASV on GO-C7Me film in 100 μM $CuCl_2$ solution. (A) pH value of the solution; (B) preconcentration time, and (C) accumulation potential.

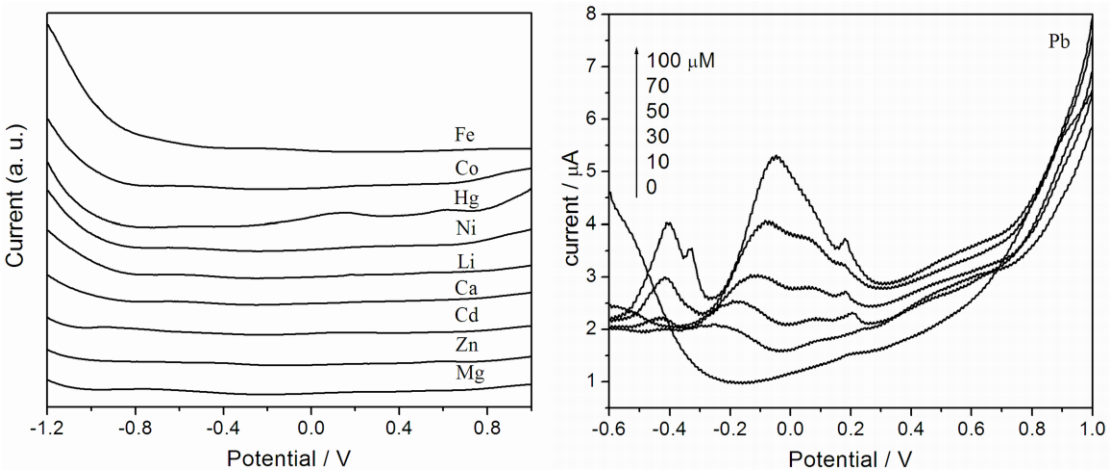

Fig. S10 SWASV responses of the GO-C7Me modified Au electrode toward other metal at 100 μM in NaAc buffer with pH of 5.3.

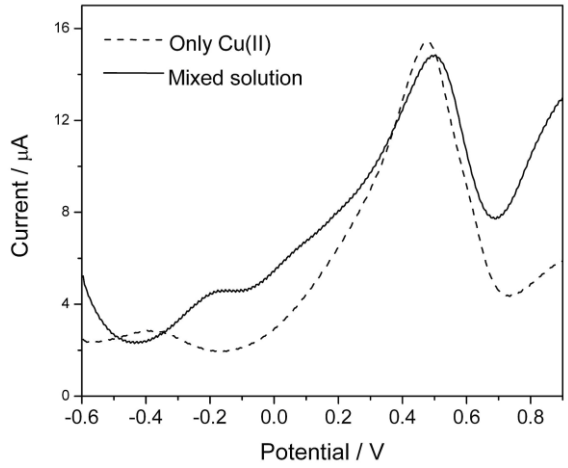

Fig. S11 SWASV response of the GO-C7Me modified electrode toward Cu(II) in solution containing Fe(III), Li(I), Mn(II), Ni(II), Ca(II), Mg(II), Cd(II), Na(I), Hg(II), Co(II), Zn(II), Pb(II) cations with the same concentration of 100 μM. The electrochemical stripping detection conditions are the same as in Fig. 3.

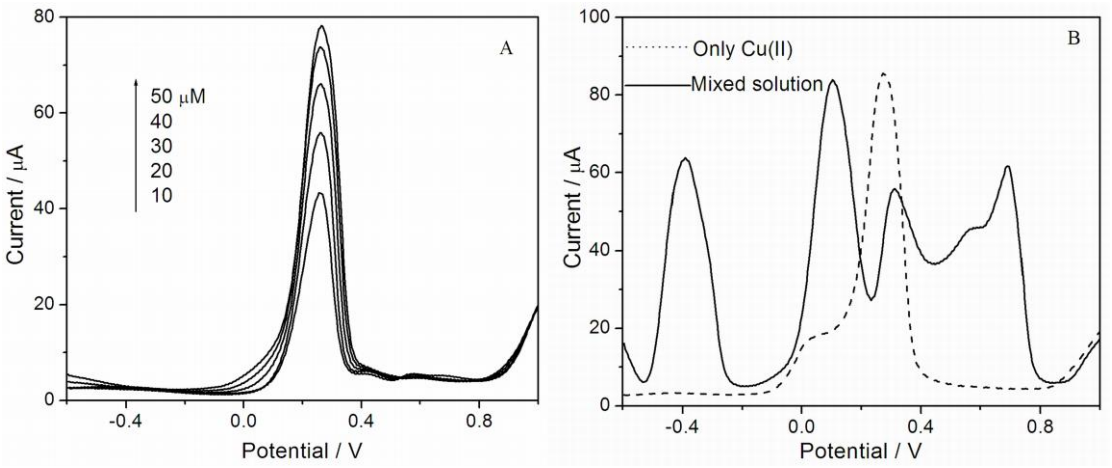

Fig. S12 (A) SWASV response of the bare Au electrode toward pure Cu(II); (B) SWASV responses of the bare Au electrode toward Cu(II) in the presence of Li(I), Mn(II), Ni(II), Ca(II), Mg(II), Cd(II), Na(I), Hg(II), Co(II), Zn(II), Pb(II) with the concentration of 100 μM. The electrochemical stripping detection conditions are the same as in Fig. 3.

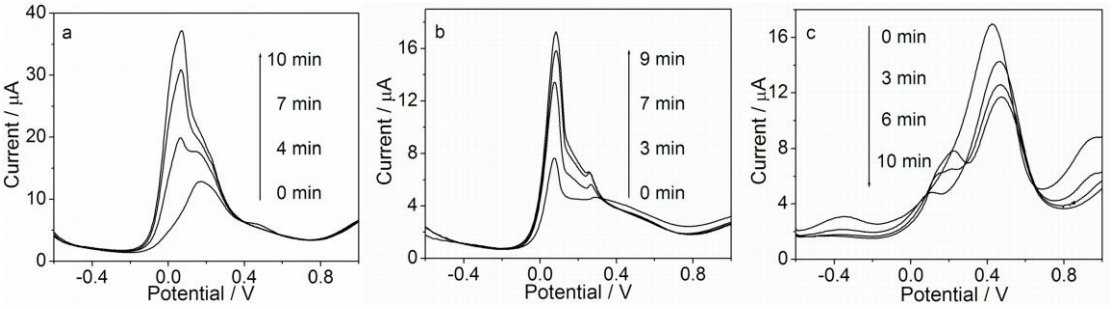

Fig. S13 SWASV response of (a) GO-C3Me, (b) GO and (c) GO-C7Me film toward Cu(II) (100 μM) at different time. The electrochemical stripping detection conditions are the same as in Fig. 3.

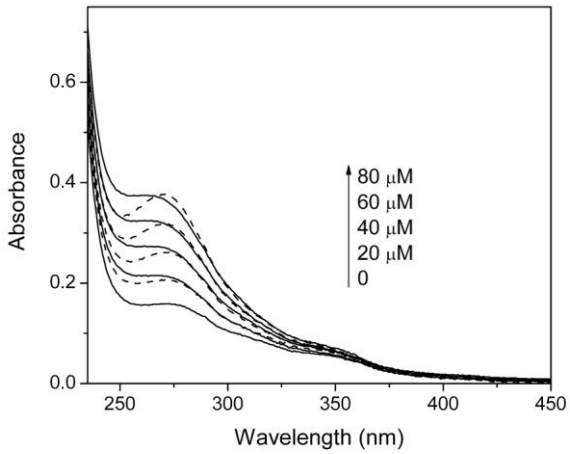

Fig. S14 The solid lines represent the change in the UV-vis spectrum of GO before and after the addition of Cu(II) at concentrations of 0, 20, 40, 60, 80 μM; The dash lines represent the overlapped absorption of GO and Cu(II) at concentrations of 0, 20, 40, 60, 80 μM.